



Efficacy of resveratrol encapsulated microsponges delivered by pectin based matrix tablets in rats with acetic acid-induced ulcerative colitis

Gandhi, H., Rathore, C., Dua, K., Vihal, S., Tambuwala, M. M., & Negi, P. (2020). Efficacy of resveratrol encapsulated microsponges delivered by pectin based matrix tablets in rats with acetic acid-induced ulcerative colitis. *Drug Development and Industrial Pharmacy*, 46(3), 365-375.
<https://doi.org/10.1080/03639045.2020.1724127>

[Link to publication record in Ulster University Research Portal](#)

Published in:

Drug Development and Industrial Pharmacy

Publication Status:

Published (in print/issue): 03/03/2020

DOI:

[10.1080/03639045.2020.1724127](https://doi.org/10.1080/03639045.2020.1724127)

Document Version

Author Accepted version

General rights

Copyright for the publications made accessible via Ulster University's Research Portal is retained by the author(s) and / or other copyright owners and it is a condition of accessing these publications that users recognise and abide by the legal requirements associated with these rights.

Take down policy

The Research Portal is Ulster University's institutional repository that provides access to Ulster's research outputs. Every effort has been made to ensure that content in the Research Portal does not infringe any person's rights, or applicable UK laws. If you discover content in the Research Portal that you believe breaches copyright or violates any law, please contact pure-support@ulster.ac.uk.



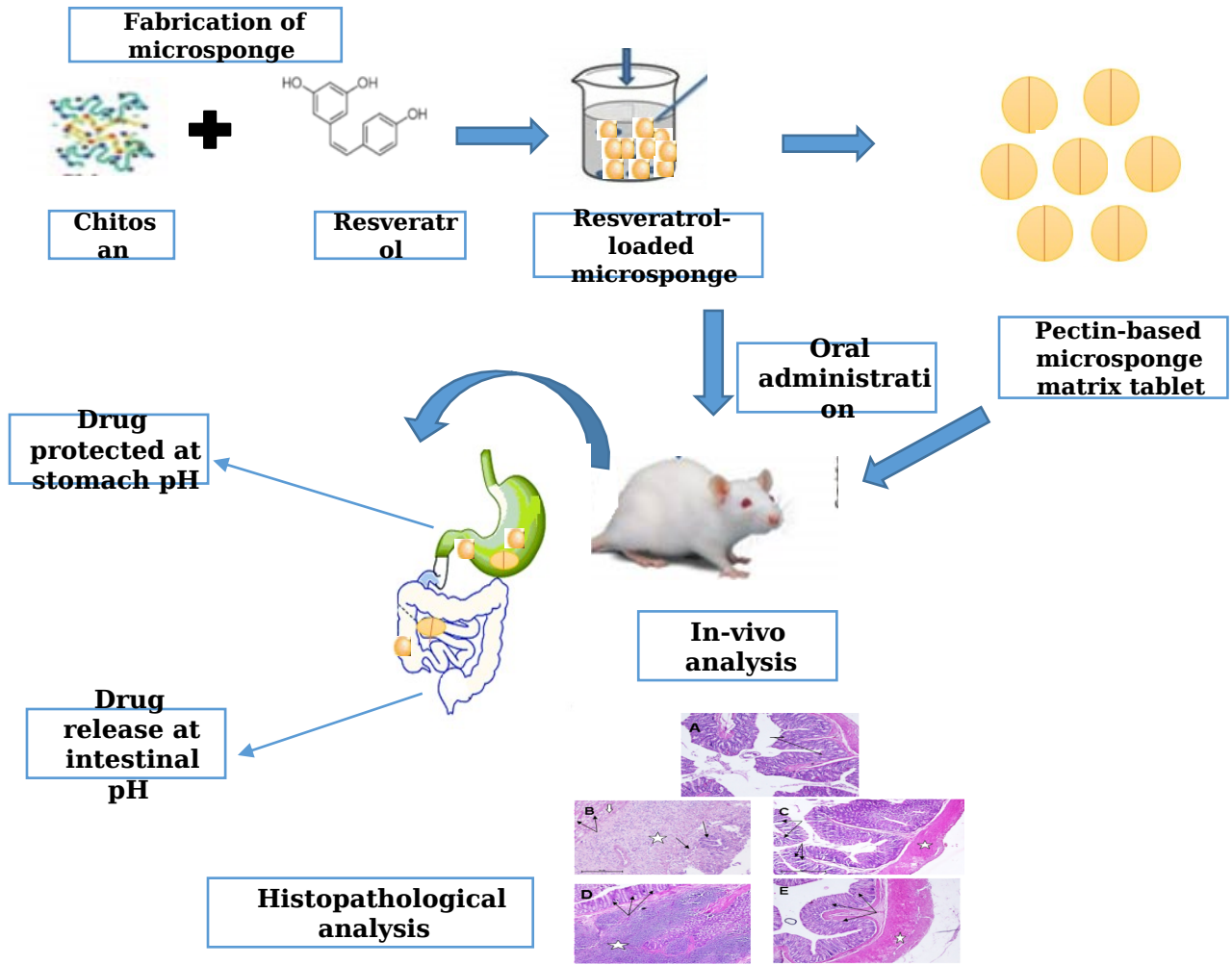
<http://jddi.tandfonline.com/doi>



Efficacy of resveratrol encapsulated microsponges delivered by pectin based matrix tablets in rats with acetic acid induced ulcerative colitis

Journal:	<i>Drug Development and Industrial Pharmacy</i>
Manuscript ID	LDDI-2019-OR-0224.R1
Manuscript Type:	Original Research Paper
Date Submitted by the Author:	10-Oct-2019
Complete List of Authors:	Gandhi, Himanshu; Shoolini University Rathore, Charul; Shoolini University Dua, Kamal; University of Technology Sydney; The University of Newcastle Faculty of Health and Medicine Vihal, Samar; Shoolini University Tambuwala, Murtaza; University of Ulster, Negi, Poonam; Shoolini University
Keywords:	Bioavailability, chitosan, Box-behnken design, quasi emulsion solvent diffusion method, ulcerative colitis, release kinetics, pectin

SCHOLARONE™
Manuscripts



1
2
3
4
5
6
7
8
9
10
11
12
13
14
15
16
17
18
19
20
21
22
23
24
25
26
27
28
29
30
31
32
33
34
35
36
37
38
39
40
41

1
2
3 1 **Efficacy of resveratrol encapsulated microsponges delivered by pectin based matrix**
4 2 **tablets in rats with acetic acid-induced ulcerative colitis**

5 3
6 4 Himanshu Gandhi¹, Charul Rathore¹, Kamal Dua^{1,2,3}, Samar Vihal¹, Murtaza M.
7 5 Tambuwala⁴ and Poonam Negi^{1*},
8 6

9 7
10 8 ¹*School of Pharmaceutical Sciences, Shoolini University of Biotechnology and Management*
11 9 *Sciences, Solan-173 212, Himachal Pradesh, India*

12 10
13 11 ²*Discipline of Pharmacy, Graduate School of Health, University of Technology Sydney,*
14 12 *Ultimo NSW 2007, Australia*

15 13
16 14 ³*School of Biomedical Sciences and Pharmacy, The University of Newcastle, Callaghan,*
17 15 *NSW 2308, Australia & Priority Research Centre for Healthy Lungs, Hunter Medical*
18 16 *Research Institute, Lot 1 Kookaburra Circuit, New Lambton Heights, Newcastle, NSW 2305,*
19 17 *Australia*

20 18
21 19 ⁴*School of Pharmacy and Pharmaceutical Sciences, Ulster University, Coleraine, Co.*
22 20 *Londonderry, United Kingdom*
23 21
24 22
25 23
26 24
27 25
28 26
29 27
30 28
31 29
32 30
33 31
34 32
35 33
36 34
37 35
38 36
39 37
40 38
41 39
42 40
43 41
44 42
45 43
46 44
47 45
48 46
49 47
50 48
51 49
52 50
53 51
54 52
55 53
56 54
57 55
58 56
59 57
60 58

29 ***To whom correspondence should be addressed**

30 Dr.PoonamNegi
31 M.S. Pharm, Ph.D
32 Professor of Pharmaceutical Science
33 School of Pharmaceutical Science
34 Shoolini University, Solan173212, India
35 E-mail: poonamgarge@gmail.com
36
37
38
39

Abstract

Objectives: The objective of the present work to encapsulate the resveratrol (RES) inside the chitosan-based microsponges, employing the systematic optimization by 3³ Box-Behnken design for the colonic targeting.

Significance: Enhanced therapeutic efficacy of RES-loaded microsponges and matrix tablets, *vis-a-vis* pure RES for ulcerative colitis.

Methods: RES-loaded microsponges were prepared employing the systematic optimization by 3³ Box-Behnken design for the colonic targeting. The best-optimized RES-loaded microsphere was compressed in the form of a tablet, employing pectin as a matrix-forming material. The encapsulation of RES inside microsphere was confirmed by XRD, DSC and FT-IR. Further, both RES-loaded microsponges and matrix tablets were evaluated for *in vitro* release kinetics and further evaluated for *in vivo* ulcerative colitis animal model.

Results: Optimization experiments was obtained as the high value of r^2 (particle size = 0.9999; %EE= 0.9652; %CDR = 0.9469) inferred excellent goodness of fit. SEM revealed nearly spherical and porous nature of RES-loaded microsponges. The *in vitro* release kinetic showed zero-order release for RES-loaded microsponges and Korsmeyer-Peppas model for matrix tablets. The pharmacodynamic studies, in ulcerative colitis rat model, indicated better therapeutic efficacy of drug-loaded microsponges and matrix tablets, *vis-a-vis* pure RES. Thus, the present study advocates the potential of RES based microsponges delivered by pectin based matrix tablet, in the treatment of various colonic disorders.

Conclusion: The present study proved that RES-loaded microsponges and matrix tablets based on chitosan and pectin, can be the ideal delivery system for colonic delivery of RES.

1
2
3 73 **Keywords:**Chitosan;Box-behndesign;quasi emulsion solvent diffusion method; pectin;
4
5 74 ulcerative colitis; release kinetics.
6

7 75 **Introduction**

8
9 76 Resveratrol (RES) (3,5,4'-trihydroxystilbene), is a non-flavonoid polyphenolic phytoalexin
10
11 77 molecule, synthesized by various plant species like grapes, berries, and peanuts, in response
12
13 78 to stress and microbial infections[1, 2]. RES acts as a strong antioxidant by inhibiting reactive
14
15 79 oxygen species (ROS) primarily by activating protein kinase and suppresses cyclooxygenase
16
17 80 (COX-2), and lipid peroxidation. It has demonstrated its therapeutic roles as anti-
18
19 81 inflammatory, analgesic, cardio-protective, neuroprotective, chemo-preventive, and anti-
20
21 82 aging agents [3]. There are many reports available for its decent therapeutic efficacy for
22
23 83 lower gastrointestinal (GI) diseases like ulcerative colitis, peptic ulcer, Crohn's diseases and
24
25 84 colon cancer [4, 5]. Despite of high oral absorption (~ 75%), the oral bioavailability of RES
26
27 85 is less than 1%, due to its extensive intestine and liver metabolism [6, 7]. Moreover, rapid
28
29 86 absorption in the upper GI tract and pre-systemic metabolism subsequently results in the
30
31 87 lower amount of drug reaching to the colon [8, 9]. Thus, there is a necessity to develop an
32
33 88 efficient drug delivery system for RES, which would be able to target the drug directly to the
34
35 89 colon and prevent its release in the upper GI tract.

36
37 90 Novel drug delivery carrier systems *viz.* nanoparticles, nano-spheres, micro-particles,
38
39 91 microspheres, beads and micro/nano-sponges based on various polymers, have been
40
41 92 consumed for colon-specific drug delivery[10-13]. These systems are, controlled by GI transit
42
43 93 time, GI pressure differences, GI pH differences, and colonic bacterial enzymes [14]. In the
44
45 94 recent past, polysaccharides that are particularly metabolised by the colonic flora have
46
47 95 increased acceptance as a colon-specific drug delivery systems. Pectin, a linear
48
49 96 polysaccharide is extensively used as a colon-specific matrix carrier due to some attractive
50
51 97 features, *viz.* hydrophobicity, and ability to form gel, biodegradability, and persistence to
52
53 98 intestinal enzymes. The other polymer in the polysaccharide class is chitosan, which is pH-
54
55 99 sensitive and is used as a colon-specific carrier owing to its ability to restrict the drug release
56
57 100 in the gastric pH, and significantly release the drug at higher pH [15]. Based on the above
58
59 101 considerations, the advantages of both chitosan and pectin for colon-specific delivery of RES
60
102 were combined into a unit dosage form, wherein chitosan was employed in the form of
103 microsponges, and pectin as a matrix-forming material. Microsponges have the competency
104 to encapsulate and adsorb a high degree of active ingredients onto its surface owing to
105 numerous interconnected pores. Apart from high drug entrapment, and site-specificity,

1
2
3 106 microsponges have a specific property of retaining on the surface of the colon, and thereby,
4 107 increase the absorption of the drug in the colon [16, 17]. Further, it can prevent the drug from
5 108 early absorption, as the drug is enclosed inside the micro-sponge, and also the frequency of
6 109 dosing may be decreased *via* controlled delivery of drug over a longer period of time, and
7 110 hence the patient compliance [18].
8
9

10
11
12 111 Polymeric erosion based matrix systems comprising of hydrophilic polymer is highly popular
13 112 in tablet manufacturing for controlled release application. Such matrix system, retard the drug
14 113 release, owing to the formation of the gelatinous surface layer due to swelling in the aqueous
15 114 medium, which controls the diffusion of water when placed in an aqueous medium[19, 20].
16 115 The present work was designed to systematically optimize the RES-loaded chitosan
17 116 microsponges employing Box-behnken design with respect to particle size, entrapment
18 117 efficiency, and percent cumulative drug release. The best-optimized RES loaded microsphere
19 118 formulation was developed into the erosion based matrix tablet employing pectin. Finally, all
20 119 the RES formulations were evaluated employing an acetic-acid induced ulcerative colitis
21 120 model in rats.
22
23
24
25
26
27
28
29

30 121 **Experiment**

31 122 ***Materials***

32
33
34
35 123 RES was received *ex gratis* from Tirupati Medicare Ltd., PaontaSahib, Sirmaur, Himachal
36 124 Pradesh, India. Acetone, sodium chloride, polyvinyl alcohol (PVA), sodium dihydrogen
37 125 phosphate, potassium dihydrogen phosphate, sodium hydroxide (NaOH), and pectin, were
38 126 procured from Nice Chemical Pvt. Ltd., Cochin, India. Ethanol, and HCl were purchased
39 127 from Merck Specialties Pvt. Ltd., Mumbai, India, while Span 80, was purchased from
40 128 Qualikems Laboratory Reagents, New Delhi, India. Chitosan was purchased from Hi-Media
41 129 Laboratory Pvt. Ltd., Mumbai, India, while, PVP K30, and microcrystalline cellulose (MCC),
42 130 were obtained from Loba Chemical Pvt. Ltd., Mumbai, India.
43
44
45
46
47
48
49

50 131 ***Methods***

51 132 ***Fabrication and evaluation of microsponges***

52
53
54
55 133 Microsphere preparation was done by quasi-emulsion technique as previously reported by
56 134 authors [21]. Methanol was employed as a solvent to dissolved RES. 0.1 mL of internal
57 135 aqueous phase was added into the organic phase to form w/o primary emulsion. Herein, the
58
59
60

1
2
3 136 internal phase comprised of 1% (w/v) aqueous solution of NaCl (as porogen) and Span 80.
4
5 137 The organic phase was prepared in the DCM. Separately, chitosan was dissolved in minimum
6
7 138 amount of 1% w/v aqueous solution of the glacial acetic acid solution, and RES was
8
9 139 dissolved in methanol. Both the solution was then added to the required volume of DCM to
10
11 140 form the organic phase. Finally, primary w/o emulsion was added into 5% w/v aqueous PVA
12
13 141 (external phase), to form w/o/w double emulsion. The prepared emulsion was then,
14
15 142 continuously stirred for 2h on a mechanical stirrer. Microsponges so prepared were filtered,
16
17 143 dried at 60°C, and stored in the desiccator until further use[22].

18 144 *Systematic optimization of microsponges as per the experimental design*

19
20 145 RES-loaded microsponges were optimized employing three factor three-level, Box–Behnken
21
22 146 design (BBD). The dependent variables were the amount of RES (X1), polymer (X2), and
23
24 147 solvent (X3), used at three different levels of each variable, viz. low (-1), intermediate (0),
25
26 148 and high (+1). Various microsphere formulations (Table 1) prepared as per the design were
27
28 149 investigated for the response variables like particle size, percent cumulative drug release (%
29
30 150 CDR), and percent entrapment efficiency (%EE) as the response variables.

31 151 *Characterization of microsponges*

32 33 152 *Particle size determination*

34
35
36 153 The mean particle size of microsphere was analysed by Malvern Master Sizer (Scinrocco,
37
38 154 2000), installed at the University Institute of Pharmaceutical Sciences (UIPS), Chandigarh,
39
40 155 India. All the samples were diluted 50 times before analysis. The samples were then placed
41
42 156 into cuvettes and the intensity of fluctuation of the laser beam was recorded and interrelated
43
44 157 with the particle size of the dispersed phase[23].

45 158 *Entrapment efficiency (%EE), percentage yield (%Y) and percentage drug loading(%DL)*

46
47
48 159 For %EE, microsphere equivalent to 10 mg of the drug were crushed and extracted
49
50 160 employing methanol by ultra-sonication. To separate the insoluble residue, centrifugation was
51
52 161 then carried out at 2000 rpm for 10 min. The supernatant was analysed by the U.V
53
54 162 spectrophotometer (Systronics-Model-2202) at λ_{\max} 302 nm after appropriate dilution [24]. To
55
56 163 determine the concentration of RES, the value of absorptivity used was 1437. The amount
57
58 164 of % EE, % Y and %DL was calculated employing the following Equations (1),(2) and (3)
59
60 165 respectively.

$$166 \quad \%E = \frac{\text{Mass of the drug in microsp sponge}}{\text{Initial mass of the drug}} \times 100(1)$$

$$167 \quad \%Y = \frac{\text{Mass of the drug in microsp sponge}}{\text{Initial mass of the drug} + \text{Initial mass of polymer}} \times 100(2)$$

$$168 \quad \%DL = \frac{\text{Mass of the drug in microsp sponge}}{\text{Mass of microsp sponge}} \times 100(3)$$

169 ***In vitro drug release***

170 *In vitro* dissolution study of RES for a period of 12 h, from all the prepared microsp sponge
171 formulations, was carried out employing the USP–Type-II dissolution
172 apparatus(ElectrolabETC 11LX) [25]. Microsponges equivalent to 10 mg of the RES, was
173 placed in the jar, and the study was performed at different pH, i.e. pH 1.2 (200mL), for 2 h,
174 pH 6.8 for 2-6 h and pH 7.4 (700 mL) for subsequent hours i.e., 6-12 h to simulate the same
175 conditions of GIT. The stirring was maintained at 100 rpm at 37±5°Ctemperature. Samples (5
176 mL) were withdrawn periodically at regular time intervals (0, 0.5 1.5, 2, 3, 4, 6, 8,10, 12h)
177 while an equal volume of fresh medium was added to maintain the sink conditions. The
178 samples were diluted with methanol and analysed spectrophotometrically at λ_{max} 302 nm to
179 calculate the percent cumulative drug release (%CDR) values [26].

180 ***Optimisation data analysis and validation***

181 The optimization and validation of data obtained for various response variables *viz.*, particle
182 size, %EE, and %CDR were performed employing mathematical modelling. The second-
183 order quadratic polynomial model was selected using multiple linear regression analysis
184 (MLRA) to study the probability of a significant interaction(s) among the response
185 variables[27, 28]. The response surface analysis was studied employing three dimensional
186 (3D) response surface plots, and two-dimensional (2D) contour plots, constructed using
187 Design Expert® ver.10.0.1 (Stat-Ease Inc., Minneapolis, MN). The numerical optimization
188 using desirability function by ‘trading off’ of the response variables was employed to select
189 the optimum microsp sponge formulation (RES:340 mg; polymer; 455 mg). A total of ten
190 check-point microsp sponge formulations were selected and evaluated. The observed and
191 predicted values for the studied responses, i.e. particle size, %CDR and %EE, were critically
192 compared. Percent bias (percent error) was determined with respect to the observed responses
193 and the residual plots were also generated.

194 ***Characterization of the optimized microsp sponge formulation***

195 ***Scanning electron microscopy***

196 To observe the surface of micro sponge, dried samples were mounted on a metal stub using
197 double-sided adhesive tape and sputter-coated with gold for 1 min. under vacuum and then
198 observed under a scanning electron microscope (SEM) at 10 kV (QUANTA 250, FEI
199 Makers, Singapore), installed at IIT, Mandi, H.P, India[27].

200 ***Differential scanning calorimetric (DSC) analysis***

201 DSC (STA 449 F1 Jupiter) thermal analysis was carried out, on the optimized RES-loaded
202 micro sponge formulation, pure RES, and chitosan. Approximately 5mg sample was weighed,
203 and sealed into aluminium pans. All the samples were heated at the rate of 10°C/min in a
204 temperature range of 25-300°C, in nitrogen atmosphere [29].

205 **Thermal gravimetric analysis (TGA)**

206 TGA (STA449F1 Netzsch) thermal analysis was carried out, on the optimized RES-loaded
207 micro sponge formulation, pure RES, and chitosan. Approximately 5mg sample was weighed,
208 and sealed into aluminum pans. The experiment was conducted in temperature range of 25-
209 300°C at a heating rate of 10°C/min in a temperature range of 25-300°C, in a nitrogen
210 atmosphere (20 ml/min) [29, 38].

211 ***X-ray powder diffraction (XRD) study***

212 XRD was recorded to characterize the crystal and physical state of micro sponge, pure RES
213 and chitosan. The instrument (SmartLab 9kW rotating anode x-ray diffractometer) was
214 operated at a voltage of 45mV and current 20A, and the diffraction patterns over a range of 5-
215 10°C/min in terms of 2 θ [29].

216 ***Formulation and evaluation of colon-targeted matrix tablet***

217 Colon targeted matrix tablets of optimized RES-loaded microsponges were prepared by direct
218 compression method. Pectin (150 mg, matrix diluent), optimized micro sponge formulation
219 (150 mg), polyvinyl pyrrolidone (PVPk30) (binder, 150 mg), and microcrystalline cellulose
220 (MCC, 50 mg) were accurately weighed and mixed uniformly to form a homogenous
221 powder-mixture. The final mixture was then passed through sieve no. 22, and was directly
222 compressed into tablets, employing Rotatory tablet punching machine (Cadmech. Pvt.

223 Ltd.)[30].Tablets were evaluated for various pharmacopoeial (weight variation, friability and
224 *in vitro* dissolution) and non- pharmacopoeial (hardness) aspects.

225 The *in vitro* dissolution of the matrix tablets was done as describes in section 2.4.3. The
226 weight variation of the matrix tablets was determined as per Indian Pharmacopoeia [31].
227 Briefly, twenty tablets were weighed and the average weight was calculated. The percentage
228 of weight variation was also determined by using the following formula as shown in the
229 Equation. (4)

$$230 \quad \% \text{ Weight Variation} = \frac{\text{Individual weight} - \text{Average Weight}}{\text{Average Weight}} \times 100(4)$$

231 The friability of prepared matrix tablets was determined with Roche type friabilator. 10
232 tablets were weighed and tested at a speed of 25 rpm for 4 min. After the process was
233 stopped, tables were removed out of the friabilator then after, dust was wiped-off, and tablets
234 were weighed again. The difference between the weight before, and after, the process, was
235 determined. The percentage friability (%) was calculated using the following Equation (5)

$$236 \quad \% \text{ Friability} = \frac{\text{Tablet weight before} - \text{Tablet weight after}}{\text{Tablet weight after}} \times 100(5)$$

237 The hardness of the prepared matrix tablets was determined to employ Monsanto hardness
238 tester. The hardness was measured in terms of force (Kg/cm²), required to break the tablet.
239 The tablet was placed between two anvils, the force was applied, until the tablet breaks and
240 this force was recorded. The hardness test was performed on twenty tablets, and the average
241 hardness was recorded [31].

242 ***In vitro drug release kinetics***

243 Release data from the best-optimized microsponge formulation and its matrix tablet were
244 fitted to various mathematical models to study the drug release mechanisms. The various
245 models employed were zero-order (% cumulative drug release vs. time) Equation(6), first-
246 order (log % drug release vs. time) Equation (7), Higuchi model (% cumulative drug release
247 vs. square root of time) Equation(8), and Peppas model (log % drug release vs. log time)
248 Equation(9). The kinetic model was selected based on best fit with the highest value of the
249 regression coefficient (r²) [7, 21].

$$250 \quad Q_t = k_0 t \quad (6)$$

$$\ln Q_t = \ln Q_0 + k_1 t \quad (7)$$

$$Q_t = k_0 \sqrt{t} \quad (8)$$

$$Q_t = k_k t^k \quad (9)$$

254

255 Here Q_t is the amount of drug released at time t , Q_0 is the initial amount of drug, whereas, k_0 ,
256 k_1 , k and k_k are the corresponding release rate constants for zero-order, first-order, Higuchi and
257 Korsmeyer-Peppas model respectively.

258 *In vivo pharmacodynamic study*

259 The animal study was carried out in prior approval of the Animal Ethical Committee, of
260 Shoolini University Animal Ethics Committee, duly approved for the purpose of control and
261 supervision of experiments on animals by the Government of India, (IAEC No/SU-
262 PHARM/7/10).

263 *Acetic acid-induced experimental ulcerative colitis in the colon*

264 Fifteen wistar albino rats (body weight = 160–200 g), were taken, and caged individually
265 with food and water *ad libitum*). The rats were distributed randomly into five groups with
266 each group comprising of three animals. Except for the negative control group, colitis was
267 induced in all the groups by intrarectal administration of 1 mL of (4%) (v/v) acetic acid,
268 which resembles with the inflammatory bowel disease (IBD). The catheter was introduced
269 into the anus up to a length of 6 cm, and then acetic acid was administered [32]. The full IBD
270 model was developed by keeping animals untreated for about three days [30]. After three
271 days, each group received the treatment orally in 0.5% carboxymethyl cellulose (w/v)
272 solution. Group 1 served as a negative control, group 2 served as colitis group without any
273 treatment, group 3 received pure RES (25mg/kg), group 4 received RES -loaded
274 microsponges (equivalent to 25mg/kg), and group 5 received RES-loaded microsphere
275 matrix tablets (equivalent to 25mg/kg) [33].

276 *Pharmacological Assessments*

277 After seven days of treatment, the animals were sacrificed and colon was removed, and based
278 on inflammatory scales, and ulcer projections were visualized. The inflammatory scales were
279 categorised as; 0 = normal coloured colon, 0.5 = red coloration, 1 = spot ulcer, 1.5 =
280 haemorrhagic streaks, and 2 = haemorrhagic ulcer.

281 *Histopathology assessment*

282 Histopathological analysis was performed by preserving the part of the colon in a 10%
283 formalin solution. These colonic sections were stained with hematoxylin and eosin (H&E)
284 and examined using a light microscope with a fitted Nikon camera for the presence of any
285 necrosis, ulceration, haemorrhage, and inflammatory cell infiltration [34].

286 **Results and discussion**

287 *Formulation and optimization of microsponges*

288 In the present research, quasi emulsion technique was used to fabricate the various RES-
289 loaded microsphere formulations. Chitosan was employed as a polymer for the preparation
290 of microsphere due to its ability to release the drug, particularly at the colonic site. The
291 prompt mixing of w/o primary emulsion and water at the interface resulted in the
292 precipitation of RES-loaded structures of chitosan. For the optimization RES-loaded
293 microspheres, a three-factor, three-level, the Box-Behnken design was employed. Table 1
294 summarises an account of the 17 experimental runs studied, along with the coded values and
295 actual values for the studied factors. Various microsphere formulations fabricated as per the
296 design were investigated for %EE, %CDR and particle size as the response variables.

297 **[Space for Table 1]**

298 *Response surface mapping and data analysis*

299 The data analysis of the response variables employing second-order quadratic polynomial
300 models [27, 28], suggested that the quadratic model was highly significant ($p < 0.05$) along
301 with the model terms ($p < 0.0001$). The special polynomial mathematical model encompassing
302 ten coefficients (β_0 - β_{33}) represent quadratic and interaction terms, as shown in
303 Equation(10).

$$304 \quad Y = \beta_0 + \beta_1X_1 + \beta_2X_2 + \beta_3X_3 + \beta_{12}X_1X_2 + \beta_{13}X_1X_3 + \beta_{23}X_2X_3 + \beta_{11}X_1^2 + \beta_{22}X_2^2 +$$
$$305 \quad \beta_{33}X_3^2 \quad (10)$$

306 A very high degree of predictive ability of the optimization experiments was obtained as the
307 value of overall bias was $0.1109 \pm 0.2253\%$. Further the high value of r^2 (particle size =
308 0.9999; %EE= 0.9652; %CDR = 0.9469) inferred excellent goodness of fit. The residual plots
309 were found to be uniform, comparatively narrow and random scatter around the zero-axis
310 [27, 35].

311 **[Space for Table 2]**

1
2
3 312 Figure 1, depicts 2D-contour plots and corresponding 3D-response surface plots for % EE
4 313 (A), %CDR (B), and particle size (C). In the current studies, polymer and drug concentration
5 314 had a greater effect on all the studied response variables, out of all the studied input variables.
6
7 315 A curvilinear dip in the values of % EE followed by an increasing trend was observed with an
8
9 316 increase in the drug concentration, and a decrease in polymer concentration as shown in
10
11 317 Figure 1A. In case of %CDR, a twisted shape curve was observed with an increase in both
12
13 318 drug as well as polymer concentration as given in Figure 1B. An increase in polymer
14
15 319 concentration negatively influenced the %CDR, while, an increase in drug concentration
16
17 320 enhanced the former. This can be attributed to the fact that the drug release from the polymer
18
19 321 matrix occurs after complete swelling of the polymer, and as the quantity of polymer in the
20
21 322 formulation increases, so the time required to swell also increases, and hence, slower the drug
22
23 323 release. In the case of particle size shown in Figure 1C, a linear relationship was obtained for
24
25 324 polymer and drug concentration. With the increase in polymer or drug concentration, particle
26
27 325 size was increased, however, the effect was more pronounced in case of polymer
28
29 326 concentration. The increase in the polymer concentration results in an increase in the
30
31 327 viscosity of the internal phase, which subsequently gives rise to the generation of more
32
33 328 viscous forces resisting droplet breakdown, and thus bigger sized particles. The search for
34
35 329 optimum microsponge formulation was carried out using numerical optimisation and
36
37 330 desirability function to get the required goals for the response variables. Table 3 presents the
38
39 331 constraint set for numerical optimisation. In model validation, a total of ten check-point
40
41 332 formulations were selected from the RSM. Hence, based on these parameters the best
42
43 333 formulation was selected and further used for characterization.

42 334 **[Space for Figure 1]**

45 335 **[Space for Table 3]**

46 336 ***Percentage yield (%Y) and Drug loading (DL)***

48 337 The %Y of all the prepared microsponges ranged between 69.45 ± 0.52 - $86.68 \pm 0.67\%$, while
49
50 338 %DL values were in the range of 40.1 ± 0.34 - $71.45 \pm 0.76\%$. With an increase in the drug
51
52 339 concentration, %Y and %DL were found to be increased. This might be due to the high drug
53
54 340 and polymer concentration, which led to increase in viscosity of the dispersed phase, and
55
56 341 reduced the diffusion rate of DCM from viscous solutions into the aqueous phase, thus
57
58 342 improving the yield and loading [36].

59 343 ***Characterization of optimized formulation***

345 ***Surface morphology***

346 The SEM image revealed formulation to be of nearly spherical shape having sufficient
347 surface porosity as shown in Figure 2a. The presence of numerous interlinked pores all over
348 the particle was also present imitating the spongy structure.

349 ***X-ray powder diffraction (XRD) study***

350 The XRD pattern of pure RES, polymer, and optimized microsp sponge formulation were
351 recorded, and the overlay-XRD spectrum is shown in Figure 2b. RES showed numerous sharp
352 and intense diffraction peaks at 13.3, 16.4, 19.2, 22.4, 25.3, 28.3 and 45.3°, which indicates
353 crystalline nature at the respective 2θ positions. The polymer chitosan did not show any
354 peaks, suggesting its amorphous nature as depicted in literature. The microsp sponge
355 formulation also did not reveal any peaks of polymer and drug, indicating the entrapment of
356 drug inside the microsponges [29].

357 ***FT-IR spectra***

358 The overlay FTIR spectra of RES, Chitosan and microsp sponge formulation is depicted in
359 Figure 2c. RES exhibited three strong absorption bands at 1611 cm^{-1} , 1588 cm^{-1} , and 1387.90
360 cm^{-1} , analogous to C-C aromatic double bond stretching, C-C olefinic stretching, and C-C
361 stretching, respectively. The peaks from 3167 to 3201 cm^{-1} depicts the O-H stretching and the
362 peak at 1561 cm^{-1} correspond to aromatic C=C bending. The peak at 1447 cm^{-1} corresponds to
363 C-C ring stretching [37]. The characteristic chitosan peaks belonging to its saccharide
364 structure at 1055 and 898 cm^{-1} and at 1655 cm^{-1} (amide I) were close to the literature value.
365 FTIR spectra of RES-loaded microsponges displayed all peaks analogous to pure RES and
366 chitosan, however, with a decreased intensity of peaks. Further, the RES-loaded
367 microsponges did not show any major peaks corresponding to the bioactive incorporated.
368 This indicates the encapsulation of the RES within the microsp sponge formulation.

369 ***Differential scanning calorimetric (DSC) analysis***

370 DSC thermograms of the drug, chitosan, and RES-loaded microsp sponge formulation are
371 shown in Figure 2d. The drug RES demonstrated an endothermic peak around 260°C, which
372 is very close to the melting point of the drug, i.e., 261°C to 263°C. Chitosan revealed an
373 endothermic peak, at around 220°C, which is close to its reported value. In the case of
374 microsp sponge formulation, there was no peak of RES and chitosan, which indicates the

complete entrapment of drug inside the micro sponge formulation and the amorphous state of micro sponge formulation [29, 38].

Thermal gravimetric analysis (TGA)

TGA thermograms of the RES-loaded micro sponge formulation, pure RES, and chitosan, are shown in Figure 2e. TGA thermograms of chitosan indicated the % weight loss of approximately 90% of the polymer ranges between 260 -290°C as shown in figure 2e (A), whereas the % weight loss of drug found to be approximately 80% ranges between 220-270°C has shown in figure 2e (B). Drug-loaded Optimized micro sponge formulation showed TGA thermogram at a temperature range between 110°C - 190°C signifying that the drug was either completely or partially changed into amorphous form [38].

[Space for Figure2]

Evaluation of RES-loaded micro sponge matrix tablets

All the evaluation parameters of matrix tables are shown in Table 4 and suggest its satisfactory characteristics. The formulations exhibited a hardness of $4.13 \pm 0.13 \text{ kg/cm}^2$ and friability below $0.69 \pm 0.23\%$ which showed satisfactory mechanical strength of the tablets. The average weight of the twenty tablets was found to be 499.65 ± 1.35 which is well within the IP limit of weight variation i.e.($\pm 5\%$).

[Space for Table4]

In vitro release of RES-loaded microsponges matrix tablets

The *in vitro* release pattern of RES, from plain microsponges, and micro sponge-matrix tablet is shown in the Figure 3. The rate of drug release in 12 h was gradually increased, with an increase in time, and then became constant or attained equilibrium, in optimized micro sponge formulation. Drug release mechanisms from micro sponge could be linked to its porous surface. The latter permits easy penetration of the release media, and its approachability to the entrapped drug. It was witnessed that the micro sponge system was able to control the drug release in gastric pH i.e., only 10% of the drug was released during an initial 2h. However, the drug release from matrix tablets at all the pH conditions was on the lower side *vis-à-vis* micro sponge formulation. This could be due to the slow swelling property of the pectin, followed by gradual erosion, and release of the drug from the matrix tablets [17, 21]. It is well reported that the drug release from a swellable hydrophilic polymer like pectin can

1
2
3 405 be controlled and relating the liquid penetration within the polymer matrix, the swelling of
4 406 the hydrated polymer, drug diffusion throughout the swollen matrix and, erosion. PVP due to
5 407 its water-soluble characteristic could help in the solubilization in the aqueous phase and helps
6 408 in the permeation of dissolution media through the matrix causing its erosion [21].
7
8
9

10
11 409 **[Space for Figure3]**
12

13 410 ***Kinetic release analysis of drug***

14
15 411 The fitting of drug release data by suitable mathematical models is a powerful tool, which not
16 412 only enables the better interpretation, and comprehension of the mechanisms involved in the
17 413 drug release process but also helps in controlling the release features according to specific
18 414 therapeutic needs. Different mathematical models as shown in Table 5 were applied to *in*
19 415 *vitro* drug dissolution profiles and their respective coefficients were estimated.
20
21
22
23
24

25 416 According to r^2 values, as shown in Table 5, it can be noted that the microsp sponge fitted better
26 417 with the zero-order kinetic model, while the microsp sponge tablets fitted best with the Peppas
27 418 model. In the Korsmeyer-Peppas model, the value of n specifies the release mechanism of the
28 419 drug as defined. For the case of spherical matrix tablets, $0.43 \leq n$ corresponds to a Fickian
29 420 diffusion mechanism, $0.43 < n < 0.85$ to non-Fickian transport, and $n > 0.85$ to super case II
30 421 transport [35]. Here, the value of n was determined to be more than 0.85, thus mimicking the
31 422 super case II transport kinetics.
32
33
34
35
36
37

38 423 **[Space for Table5]**
39

40 424 ***In vivo pharmacodynamic study***

41
42 425 After the completion of *in vivo* pharmacodynamic study, rats were sacrificed, and colon was
43 426 examined visually, on the basis of inflammatory scales as shown in Table 6 [17,40]. It is
44 427 vivid from the results that there were less colonic lesions seen in the case of treated groups
45 428 *vis-à-vis* colitis group, indicating positive therapeutic outcomes of RES, RES-loaded
46 429 microsp sponge, and microsp sponge-matrix tablets.
47
48
49
50
51

52 430 **[Space for Table 6]**
53
54 431

55 432 ***Histopathological studies***

56
57 433 All the histological pictures of various treated and untreated groups are depicted in Figure 4.
58 434 While negative control group as shown in Figure 4A, revealed healthy looking mucosal or
59
60

1
2
3 435 sub-mucosal lining, and intact mucosal crypt, acetic acid-induced colitis group (Figure 4B)
4 436 showed severe surface, and mucosal haemorrhage (white arrows), marked necrotic
5 437 alterations, and leftovers of colonic crypts (black arrows). Besides, the sub-mucosal layer in
6 438 the acetic acid-induced colitis group revealed polymorphic inflammatory cell infiltration
7 439 (stars). Thus, it can be concluded that the colitis group revealed severe mucosal ulceration,
8 440 inflammatory cell infiltration, submucosal edema, and goblet hyperplasia [40] Figure
9 441 4C pertaining to the pure RES treated group showed colonic mucosa with no haemorrhage
10 442 streak, mild preservation of crypts with slight dilations, and almost intact mucosal lining cells
11 443 (arrows). Microsponge formulation treated group, i.e. (Figure 4D), and microsponge-matrix
12 444 tablet treated group, (Figure 4E) revealed intact mucosal crypts, healthy mucosal and
13 445 submucosal lines, suggesting both the formulations to preserve the normal colonic condition.
14 446 However, RES-loaded microsponge treated group revealed much prominent results in
15 447 comparison to the microsponge-matrix tablet treated group. Overall, all the RES treated
16 448 groups exhibited the complete cure of ulcerative colitis after the 7th day [33].

17
18
19
20
21
22
23
24
25
26
27
28 449 [Space for Figure 4]

30 450 **Conclusion**

31 451
32 452 The present study successfully ratified that the chitosan microsponge were able
33 453 to entrap the RES. The systemic optimization employing BBD aided in studying
34 454 the most influential variables to select the best-optimized formulation. The *in*
35 455 *vitro* release kinetics data revealed the sustained release nature of the developed systems.
36 456 Finally, in the *in vivo* ulcerative colitis model, better therapeutic outcomes from
37 457 drug-loaded microsponge, and microsponge loaded matrix tablets were achieved
38 458 *vis-à-vis* pure RES. Overall, the present studies corroborated that the developed
39 459 microsponges matrix system based on chitosan and pectin can be the ideal
40 460 delivery system for colonic delivery of RES.

41 461 42 462 **Acknowledgements**

43 463 Analytical and instrumental facilities provided by Shoolini University is
44 464 extremely acknowledged. In addition to this, the authors appreciated the support
45 465 of SAIF Lab (Punjab University), AMRC Mandi (H..) in characterization.

1
2
3 466 **Declaration of interest**

4 467
5 468 The authors report no declarations of interest.
6 469
7 470
8 471
9 472
10 473
11 474
12 475
13 476
14 477
15 478
16 479
17 480
18 481
19 482
20 483
21 484
22 485
23 486
24 487
25 488
26 489
27 490
28 491
29 492
30 493
31 494
32 495
33 496
34 497
35 498
36 499
37 500
38 501
39 502
40 503
41 504
42 505
43 506
44 507
45 508
46 509
47 510

54 510 **References**

- 55 511
56 512
57 513 [1] KasiotisKM,Pratsinis H, KletsasD. Resveratrol and related stilbenes: their anti-aging
58 514 and anti-angiogenic properties. Food ChemToxicol. 2011;61:112-20
59
60

- 1
2
3 515 [2] Baur JA, Sinclair DA. Therapeutic potential of resveratrol: the in vivo evidence. *Drug*
4 516 *Discovery*. 2006;5(6):493–506.
- 5 517 [3] Pangeni R, Sahni JK, Ali J. Resveratrol: review on therapeutic potential and recent
6 518 advances in drug delivery. *Expert Opin Drug Deliv*. 2014;11(8):1285-1298.
- 7 519 [4] Das S, Ng KY, Ho PC. Design of a pectin-based microparticle formulation using zinc
8 520 ions as the cross-linking agent and glutaraldehyde as the hardening agent for colonic
9 521 specific delivery of resveratrol: in vitro and in vivo evaluations. *J Drug Target*.
10 522 2011;19:446-57. doi.org/10.3109/1061186X.2010.504272
- 11 523 [5] Jeong JB, Lee J, Lee SH. TCF4 is a Molecular Target of Resveratrol in the Prevention
12 524 of Colorectal Cancer. *International journal of molecular sciences*. 2015;10411-10425.
- 13 525 [6] Negi P, Aggarwal M, Sharma G, Rathore C. Niosome-based hydrogel of resveratrol
14 526 for topical applications: An effective therapy for pain related disorder(s). *Biomedicine*
15 527 *& Pharmacotherapy*. 2017;88:480–487.
- 16 528 [7] Zu Y, Zhang Y, Wang W. Preparation and in vitro/ in vivo evaluation of resveratrol-
17 529 loaded carboxymethyl chitosan nanoparticles. *Drug Delivery*. 2014;1-11.
- 18 530 [8] Das S, Ng KY. Colon-specific delivery of Resveratrol: Optimization of multi-
19 531 particulate calcium-pectinate carrier. *International Journal of Pharmaceutics*.
20 532 2010;35:20-28.
- 21 533 [9] Gabriel DP, McClements DJ. Resveratrol encapsulation: designing delivery
22 534 Resveratrol encapsulation: designing delivery systems to overcome solubility, stability
23 535 and bioavailability issues. *Trends in food science and technology*. 2014;38:88-103.
- 24 536 [10] Bonechi C, Martini S, Ciani L. Using liposomes as carriers for polyphenolic
25 537 compounds: the case of trans-resveratrol. *PLoS One*. 2011;7:1-11. doi:
26 538 org/10.1371/journal.pone.0041438
- 27 539 [11] Zu Y, Zhang Y, Wang W, Zhao X, Han X, Wang K, et al. Preparation and in vitro/in
28 540 vivo evaluation of resveratrol-loaded carboxymethyl chitosan nanoparticles. *Drug*
29 541 *Delivery*. 2016;1–11. doi:10.3109/10717544.2014.924167
- 30 542 [12] Loftsson T, Brewster ME. Pharmaceutical application of cyclodextrins. *Drug*
31 543 *solubilization and stabilization*. *J Pharm Sci*. 1996;85:1017-25. doi:
32 544 org/10.1021/js950534b
- 33 545 [13] Peng X, Xiong H, Li J. Vanillin cross-linked chitosan microspheres for controlled
34 546 release of resveratrol. *J. food chem*. 2010;121(1):23–28. doi:
35 547 org/10.1016/j.foodchem.2009.11.085
- 36 548 [14] Pando D, Gutierrez G, Coca J. Preparation and characterization of niosomes
37 549 containing resveratrol. *J Food Eng*. 2013;117:227-34.
- 38 550 [15] Ahmed RZ, Patil G, Zaheer Z. Nanosponges- a completely new nano-horizon:
39 551 pharmaceutical applications and recent advances. *Drug Dev. Ind. Pharm*.
40 552 2013;39(9):1263-72.
- 41 553 [16] Osmani RAM, Aloorkar NH. Microsponge based drug delivery system for augmented
42 554 gastroparesis therapy: Formulation development and evaluation. *Asian Journal*
43 555 *Pharmaceutical Sci*. 2015;10:442-451.
- 44 556 [17] Nief RA, Hussein AA. Preparation and Evaluation of Meloxicam Microsponges as
45 557 Transdermal Delivery System. *Iraqi Journal of Pharmaceutical Sci*. 2014;23(2).
- 46 558 [18] Srivastava R, Kumar D, Pathak K. Colonic Luminal surface retention of meloxicam
47 559 microsponges delivered by erosion based colon-targeted matrix tablet. *International*
48 560 *Journal of Pharm*. 2012;427:153-62.
- 49 561 [19] Maheshwari R, Sharma P. Microsponge Embedded Tablets for Sustained Delivery of
50 562 Nifedipine. *Pharm Nanotechnol*. 2017;5(3):192-202.
- 51 563 [20] Ashord M, Fell JT, Attwood D. An evaluation of pectin as a carrier for drug targeting
52 564 to the colon. *Journal of Control Release*. 1993;26:213- 220.

- 1
2
3 565 [21]Maestrelli F, Zerroukm N, Cirri M. Comparative evaluation of polymeric and waxy
4 566 microspheres for combined colon delivery of ascorbic acid and ketoprofen.
5 567 International Journal of Pharm. 2015;485:365–373.
6 568 [22]Kumar V, Soni GC, Prajapati SK. Sustained Release Hydrophilic Matrix Tablet of
7 569 Ibuprofen: Influence of Polymers on *In vitro* Release and Bioavailability. International
8 570 Journal of Pharmaceutical Research and Sci. 2012;1(4):69-83.
9 571 [23]RathoreC, Jain N, Garg N. Polysaccharide-microsponge based matrix tablet for colon
10 572 targeting of ketoprofen:*In vitro* and *in vivo* evidence. IJPSR. 2017;8(10):4250-4260.
11 573 [24]Perge L, Robitzer M, Guillemot C. New solid lipid microparticles for controlled
12 574 ibuprofen release: formulation and characterization study. International Journal of
13 575 Pharm. 2012;422:59–67.
14 576 [25]Shinde AJ, Paithane MB, Sawant SS. Development and Evaluation of Fenoprofen
15 577 Microsponges and its Colonic Delivery using Natural Polysaccharides. Asian Journal
16 578 of Pharmaceutical Sciences and Nanotechnol.2014;1(27):42-30.
17 579 [26]DevrimB, CanefeK.Preparation and evaluation of modified release
18 580 ibuprofenmicrospheres with acrylic polymers (eudragit®) by quasiemulsion solvent
19 581 diffusion method: effect of variables. Acta Pol. Pharm. Drug Res. 2006;63:521–534.
20 582 [27]Anwer MK, Al-Shdefat R, Ezzeldin E, AlshahraniSM,Alshetaili AS, et al.
21 583 Preparation, Evaluation and Bioavailability Studies of Eudragit Coated PLGA
22 584 Nanoparticles for Sustained Release of Eluxadoline for the Treatment of Irritable
23 585 Bowel Syndrome. Frontiers in Pharmacol.2017;8:844. doi:10.3389/fphar.2017.00844
24 586 [28]Negi P, Singh B, Sharma G. Phospholipid microemulsion-based hydrogel for
25 587 enhanced topical delivery of lidocaine and prilocaine: QbD-based development and
26 588 evaluation. Drug Deliv. 2016; 23(3);941-57. doi: 10.3109/10717544.2014.923067.
27 589 [29]Zu Y, Zhang Y, Wang W, Zhao X, Han X, Wang K and Ge Y. Preparation and *in*
28 590 *vitro/ in vivo* evaluation of resveratrol-loaded carboxymethyl chitosan nanoparticles.
29 591 Drug Delivery. 2014; 1-11.
30 592 [30]Negi P,Singh B, SharmaG..Enhanced Topical Delivery of Lidocaine*via*. Ethosomes-
31 593 Based Hydrogel: *Ex-vivo* and *In-vivo* Evaluation. Journal of Nanopharmaceutics and
32 594 Drug Deliv.2014;2(2):138-147
33 595 [31]Malipeddi VR, Awasthi R, Dua K. Formulation and evaluation of controlled-release
34 596 matrix systems of ciprofloxacin.Polim Med. 2017;47(2):101-10628.
35 597 [32]Sareen R, Nath K, Jain N. Curcumin Loaded Microsponges for Colon Targeting in-
36 598 flammatory Bowel Disease: Fabrication, Optimization, and *In vitro* and
37 599 Pharmacodynamic Evaluation. BioMed Research Int.2014;2014.
40 600 [33]Indian Pharmacopoeia (IP) 2014. Government of India Ministry of health & Family
41 601 Welfare, The Indian Pharmacopoeia commission, Ghaziabad. 2014: II: 1864-1866.
42 602 [34]TahanG, AytacE, AytakinH. Vitamin E has a dual effect of anti-infammatory and
43 603 anti-oxidat activities in acetic-acid induced colitis in rats. Can J Surg. 2011;54(5):333-
44 604 38.
45 605 [35]Murad HAS, Abdallah HM, Ali SS. Menthalongifolia protects against acetic acid
46 606 induced colitis in rats. Journal of Ethnopharm. 2016;1-22.
47 607 [36]Singh B, Kapil R, Nandi M. Developing oral drug delivery systems using formulation
48 608 by design: Vital precepts, retrospect and prospects. Expert OpinDrugDeliv.
49 609 2011;8:1341–60.
50 610 [37]Fernanda MC, Ana DS, Raul CE.Insights into the swelling process and drug release
51 611 mechanisms from cross-linked pectin/high amylose starch matrices. Asian journal of
52 612 pharmaceutical sci. 2014;9:27-34.

- 1
2
3 613 [38] Gupta A, Tiwari G, Tiwari R, Srivastava R, Rai AK. Enteric coated HPMC capsules
4 614 plugged with 5-FU loaded microsponges: a potential approach for treatment of colon
5 615 cancer. Brazilian Journal of Pharmaceutical Sciences. 2015;51(3):591-605.
6 616 [39] Esiringu F, Demiroz FT, AcarturkF. Investigation of the effect of intracolonic
7 617 melatonin gel formulation on acetic acid-induce colitis. Drug Deliv. 2014;1-9.
8 618

9
10
11 619

12
13
14 620

15
16 621

17
18 622
19
20
21
22
23
24
25
26
27
28
29
30
31
32
33
34
35
36
37
38
39
40
41
42
43
44
45
46
47
48
49
50
51
52
53
54
55
56
57
58
59
60

For Peer Review Only

List of figures legends

Figure 1. Two-dimensional contour plots and corresponding three-dimensional response surface plot depicting the effect of various input variables on; (A) Entrapment Efficiency, (B) %CDR(cumulative drug release), and (C) Particle Size.

Figure 2. a) SEM image of resveratrol-loaded microsp sponge formulation (Magnification 8000 x) **b)** XRD spectra of drug, polymer and microsp sponge formulation **c)** FTIR spectra for resveratrol, chitosan and resveratrol-loaded microsp sponge formulation **d)** Heating curves of differential scanning calorimetry (DSC) for polymer, drug and microsp sponge formulation **e)** Thermal gravimetric analysis (TGA) of polymer, drug and microsp sponge formulation.

Figure 3. Comparison of % CDR between optimized resveratrol-loaded microsp sponge formulation and resveratrol-loaded microsp sponge-matrix tablet. Each cross bar indicates average value \pm SD (n=3).

Figure 4. Histology of colonic section of (A) Normal control group, (B) Acetic acid-induced colitis group, (C) Resveratrol treated group, (D) Resveratrol-loaded microsp sponge treated group, (E) Resveratrol-loaded microsp sponge-matrix tablet treated group.

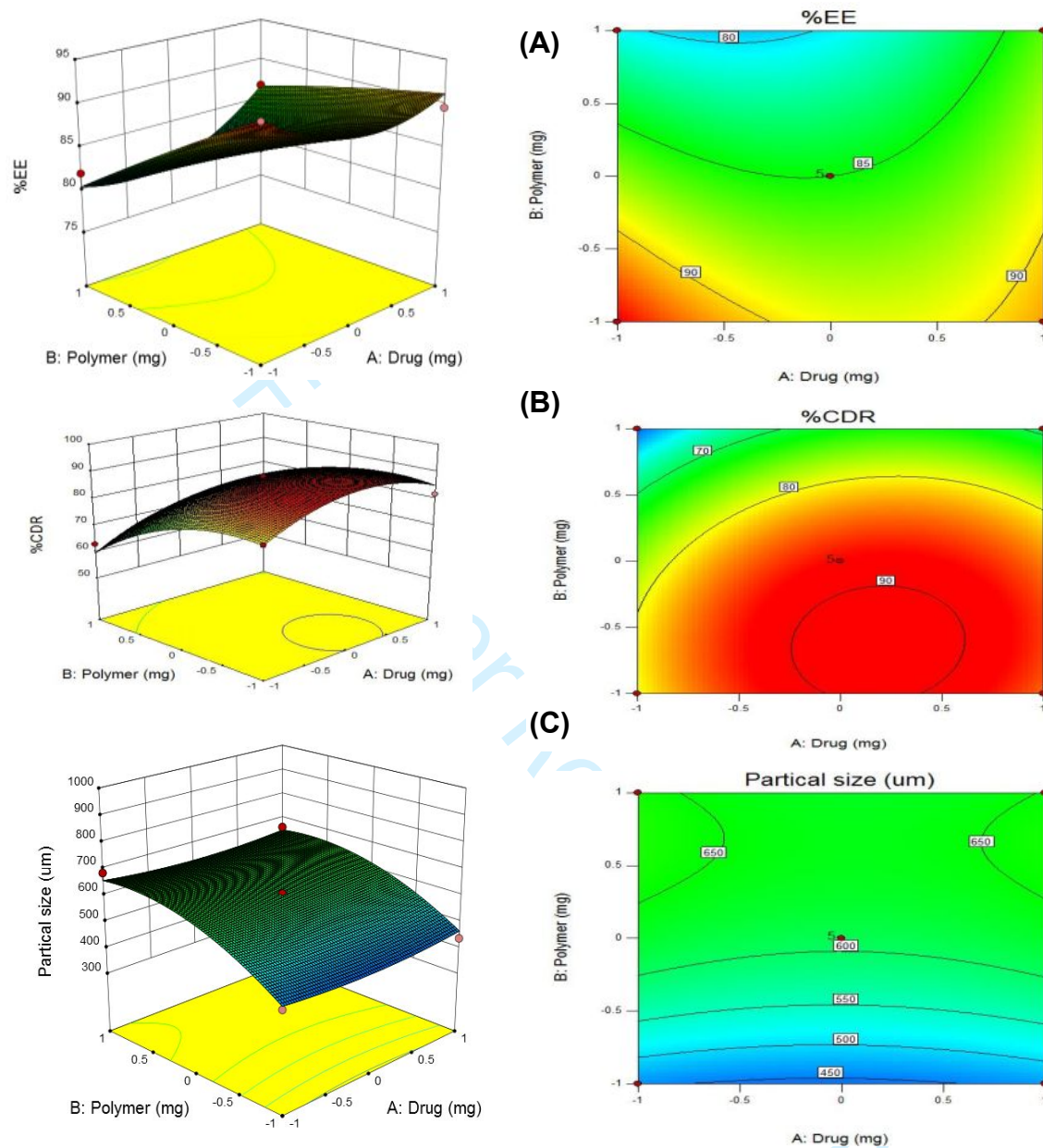
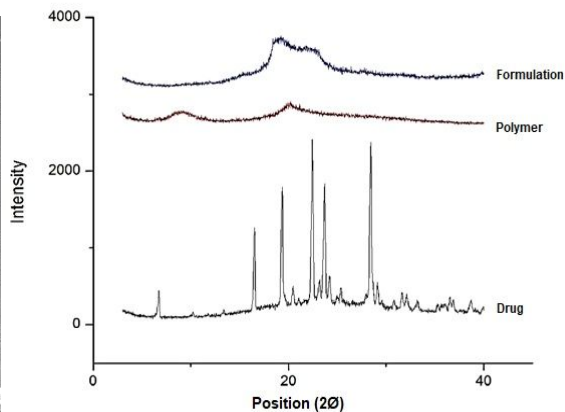
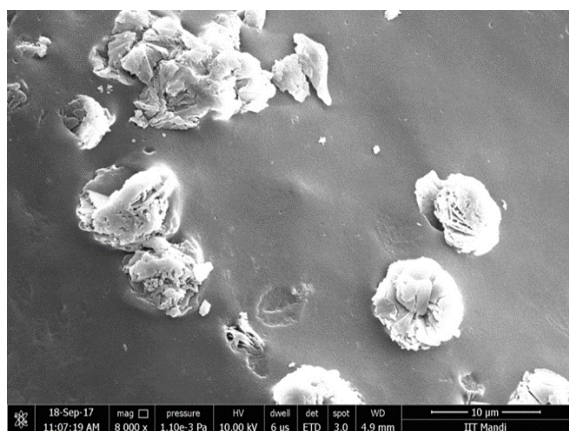
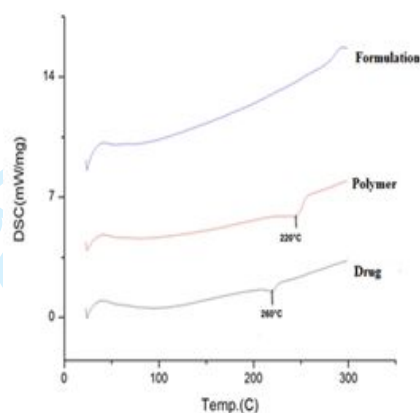
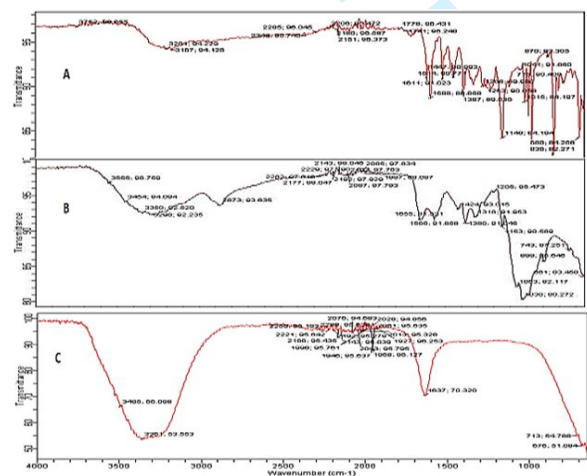


Fig. 1. Two-dimensional contour plots and corresponding three-dimensional response surface plot depicting the effect of various input variables on; (A) Entrapment Efficiency, (B) %CDR(cumulative drug release), and (C) Particle Size



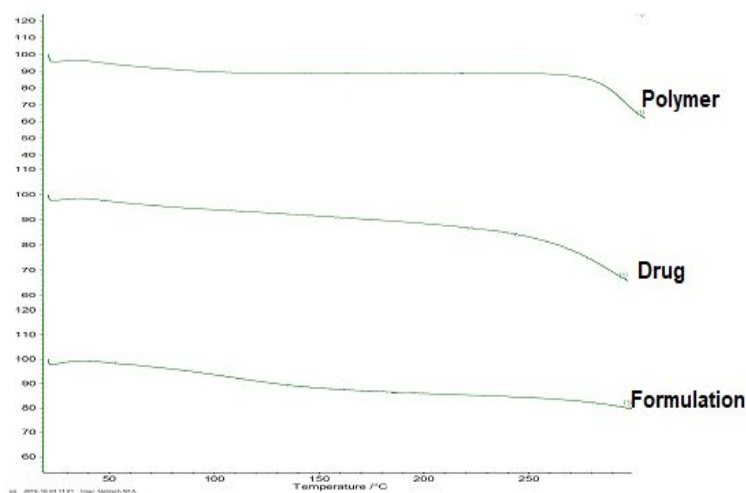
a)

b)



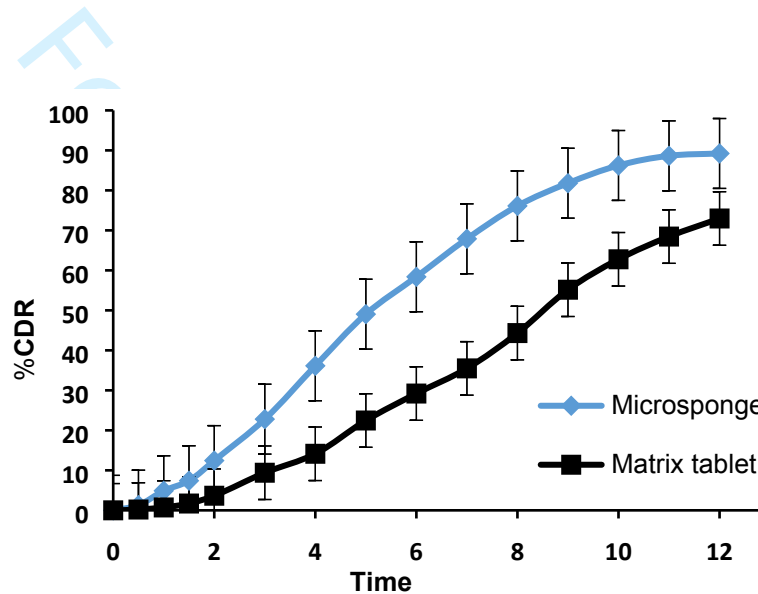
c)

d)



e)

1
2
3 **Fig. 2. a)** SEM image of RES-loaded microsp sponge formulation (Magnification 8000 x)**b)**XRD
4 spectra of drug, polymer and microsp sponge formulation **c)**FTIR spectra for A) RESB) Chitosan
5 and C) RES-loaded microsp sponge formulation **d)**Heating curves of differential scanning
6 calorimetry (DSC) for polymer, drug and microsp sponge formulation **e)**Thermal gravimetric
7 analysis (TGA) of polymer, drug and microsp sponge formulation..
8
9



18
19
20
21
22
23
24
25
26
27
28
29
30
31
32
33
34 **Fig. 3.** Comparison of % CDR between optimized RES-loaded microsp sponge formulation and
35 RES-loaded microsp sponge-matrix tablet. Each cross bar indicates average value \pm SD (n=3).
36
37
38
39
40
41
42
43
44
45
46
47
48
49
50
51
52
53
54
55
56
57
58
59
60

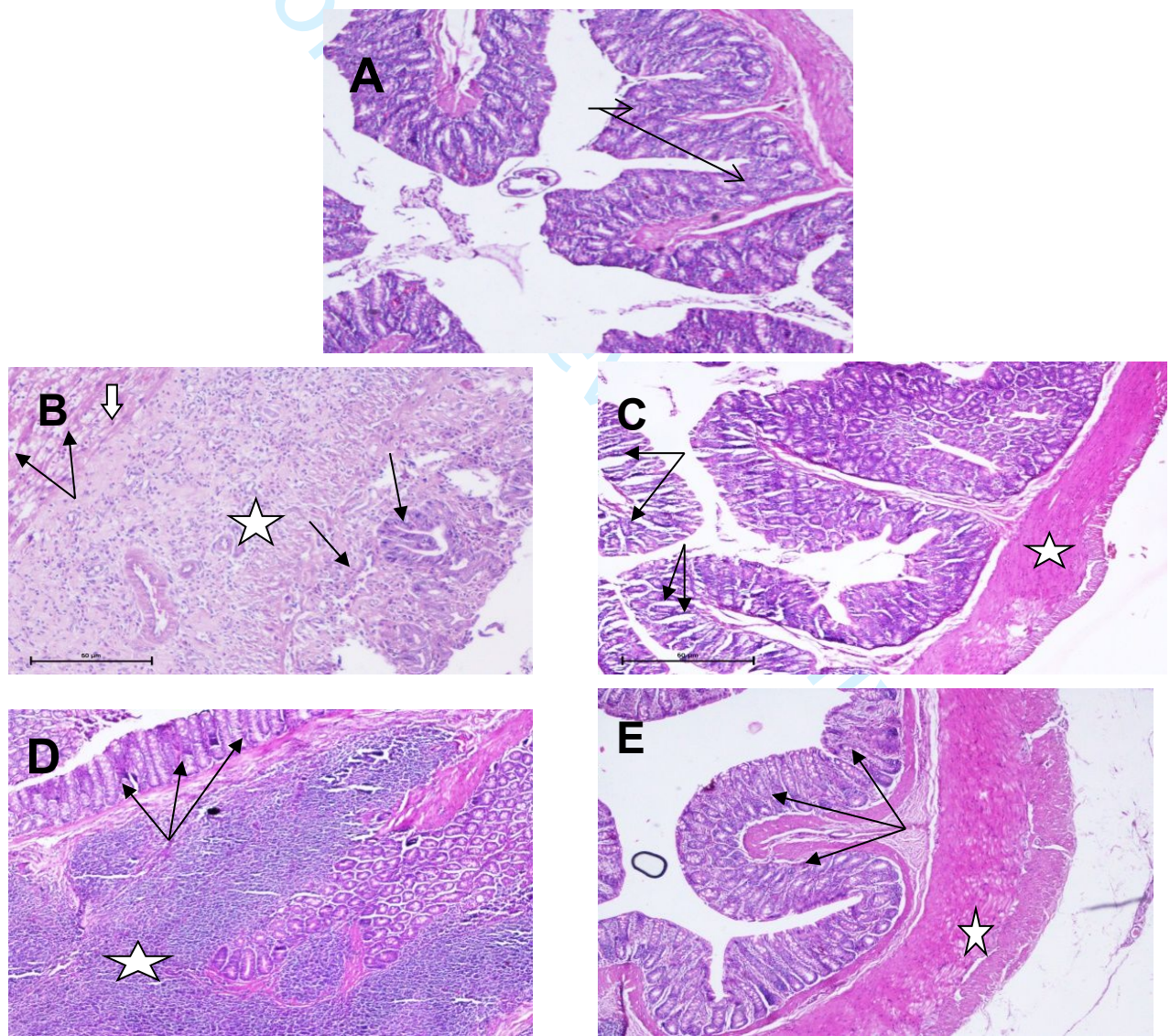


Fig. 4. Histology of colonic section of (A) Normal control group, (B) Acetic acid-induced colitis group, (C) RES treated group, (D) RES-loaded microsponge treated group, (E) RES-loaded microsponge-matrix

1
2
3 tablet treated group. **White arrow** indicates severe surface, and mucosal haemorrhage, **Black arrow**
4 indicates marked necrotic changes, and remnants of colonic crypts and **Star** indicates the sub-mucosal
5 layer revealing polymorphic inflammatory cell infiltration
6
7
8
9
10
11
12
13
14
15
16
17
18
19
20
21
22
23
24
25
26
27
28
29
30
31
32
33
34
35
36
37
38
39
40
41
42
43
44
45
46
47
48
49
50
51
52
53
54
55
56
57
58
59
60

For Peer Review Only

List of tables**Table 1:** Experimental runs of BBD design matrix and their responses**Table 2:** Polynomial mathematical model data**Table 3:** Constraints for numeric optimization and predicted solutions**Table 4:** Various evaluation parameters of matrix tablets**Table 5:** Regression coefficient values of microspunge matrix tablet and microspunge formulation**Table 6:** Macroscopic evaluation of colonic lesions of rat (0 = normal coloured colon, 0.5 = red coloration, 1 = spot ulcer, 1.5 = haemorrhagic streaks, and 2 = haemorrhagic ulcer)

Table 1. Experimental runs of BBD design matrix and their responses

Runs	Drug (mg)	Polymer (mL)	Solvent (mL)	%EE	%CDR	Particle size (μm)
1	-1	0	-1	82.8	68.47	464.172
2	1	1	0	8	68.88	663.563
				6.8		
3	0	0	0	85	88.18	609.211
4	0	0	0	85	88.18	609.211
5	1	0	-1	83	81.74	471.391
6	0	1	-1	76	56.96	378.227
7	-1	-1	0	94	80.30	446.452
8	-1	0	1	87	70.71	853.771
9	1	-1	0	89.6	81.8	436.582
10	0	0	0	85	88.18	609.211
11	0	1	1	79	72.48	923.211
12	0	0	0	85	88.18	609.211
13	-1	1	0	82	62.97	686.98
14	1	0	1	93	78.52	869.236
15	0	-1	-1	84.6	87.61	395.606
16	0	0	0	85	88.18	609.211
17	0	-1	1	92	84.64	600.834
Independent variables				Level used, actual (coded)		
				Low (-1)	Medium (1)	High (+1)
Drug				250	375	500
Polymer				250	375	500
Solvent				2.5	5	7.2

Runs	Drug (mg)	Polymer (mL)	Solvent (mL)	%EE	%CDR	Particle size (μm)
1	-1	0	-1	82.8	68.47	464.172
2	1	1	0	8	68.88	663.563
				6.8		
3	0	0	0	85	88.18	609.211
4	0	0	0	85	88.18	609.211
5	1	0	-1	83	81.74	471.391
6	0	1	-1	76	56.96	378.227
7	-1	-1	0	94	80.30	446.452
8	-1	0	1	87	70.71	853.771
9	1	-1	0	89.6	81.8	436.582
10	0	0	0	85	88.18	609.211
11	0	1	1	79	72.48	923.211
12	0	0	0	85	88.18	609.211
13	-1	1	0	82	62.97	686.98
14	1	0	1	93	78.52	869.236
15	0	-1	-1	84.6	87.61	395.606
16	0	0	0	85	88.18	609.211
17	0	-1	1	92	84.64	600.834
Independent variables				Level used, actual (coded)		
				Low(-1)	Medium(1)	High(+1)
Drug				250	375	500
Polymer				250	375	500
Solvent				2.5	5	7.2

Table 2. Polynomial mathematical model data

Coefficient code	Second-order Polynomial coefficients for response variables

	%EE	%CDR	Particle size
β_0	85	88.18	609.211
β_1	0.825	3.5275	-0.07537
β_2	-4.55	-9.1325	96.58588
β_3	3.075	1.4125	193.4795
β_{11}	2.3	1.1025	-3.38675
β_{22}	1.45	-1.2975	4.5615
β_{33}	-1.1	4.6225	84.984
β_{12}	3.325	-7.59375	20.90563
β_{13}	-0.225	-7.09875	-71.7224
β_{23}	-1.875	-5.65875	37.02588
R^2	0.9234	0.9060	0.9784

Table 3. Constraints for numeric optimization and predicted solutions

Variable	Goal	Lower limit	Upper limit	Importance
Drug (A)	In range	-1	1	***
Polymer (B)	In range	-1	1	***
Solvent (C)	In range	-1	1	***
%EE	In range	85.00	94.00	****
%CDR	In range	56.96	88.18	****
Particle size	In range	378.22	923.39	****

A	B	C	%EE	%CDR	Particle size	Desirability

0.36	0.82	0.15	88.89	89.07	463.962	1.000	Selected
-------------	------	------	-------	-------	---------	-------	-----------------

Table 4. Various evaluation parameters of matrix tablets

Parameter	Value
Average weight (n=20) mg	499.65 ±1.35
Friability test (%) (n=10)	0.69±0.23%
Hardness (n=5) (Kg/cm ²)	4.13±0.13

Table 5. Regression coefficient values of microspunge matrix tablet and microspunge formulation

Kinetic models	Regression coefficient (r²)	
	Matrix tablet	Microspunge formulation
Zero order kinetic	0.9547	0.9691
First order kinetic	0.8339	0.5933
Higuchi model	0.735	0.8631
Peppas model	0.9894	0.7661

Table 6. Macroscopic evaluation of colonic lesions of rat

Groups	0	0.5	1	1.5	2
Control	–	1	2	5	1
Resveratrol	–	1	–	2	–
Microspunge	–	2	1	-	–
Matrix Tablet	–	3	2	-	–